



## sdg-IBM1 Calculations for Osmium Nuclei

Bilal R. Obaid<sup>1</sup>, Saad N. Abood<sup>1</sup>, Laith Ahmed Najam<sup>2</sup>

<sup>1</sup>Physics Department College of Science AL-Nahrain University, Baghdad, IRAQ

<sup>2</sup>Physics Department, College of Science, Mosul University, Mosul, IRAQ



IN the framework of the sdg-interacting boson model (sdg-IBM1), we study the nuclear structure of Os isotopes. Recent calculations of E2 and E4 transitions in the Os isotopes that can not be clarified in the sd-boson models need this extension. We illustrate how gamma-unstable and triaxial shapes arise from special Hamiltonian sdg- model choices and explore ways to restrict the number of free parameters through conditions of consistency and coherence. Os nuclei, a satisfactory explanation of E2 and E4 properties is obtained, which also predicts complex shape transitions in these isotopes.

**Keywords:** Interacting Boson Model, Energy Levels,  $B(E2)$ ,  $Q(J_i^+)$ ,  $B(M1)$

### Introduction

One of the most difficult tasks for collective models of nuclei has been the classification of transitional nuclei. The triaxial nature of their energy surface, which is neither  $\gamma$ -rigid as in the Davydov-Filippov model [1] nor  $\gamma$ -unstable as in the Wilets-Jean model [2], is a complicating characteristic of these nuclei, but  $\gamma$ -soft, which requires the introduction of more elaborate geometric models such as the generalized collective model [3]. More recently, the Interacting Boson Model (IBM) [4] has provided the transitional nuclei with a very basic explanation based on the O(6) limit and its perturbations [5,6]. The O(6) limit was particularly effective in explaining the E2 transition between low-lying Pt isotope levels [5,6]. Its main disadvantages are (i) the energy surface is unstable, leading to too much staggering in the quasi- $\gamma$  band [7], (ii) the quadrupole moments disappear [8], (iii) the  $B(E2)$  values drop too quickly due to the boson cut-off [9], (iv) the E4 properties are not described [10-18]. Within the standard IBM (i.e., sd-bosons with one- and two-body interactions), none of the above issues could be satisfactorily solved and the model needs to be expanded. The easiest way to achieve this is to introduce interactions of higher order that could be motivated as a result of

g-boson renormalization. While this may resolve a specific problem, e.g., a special choice of cubic interaction introduces a  $\gamma$ -soft component in the energy surface and thus addresses the staggering problem (i) [ref.7], it is not simple to solve all the above problems (i)-(iv) in a consistent way. A second extension includes the degree of freedom of the proton-neutron (IBM-2) that for example, solves the issue of the quadruple moment (ii) [ref.19], but fails in other aspects. Another addition strongly implied by the above points (iii) and (iv) is the inclusion of the g-boson.

A detailed collection of experimental data indicating the need to include the g-boson in the IBM calculations is now available [see ref.5 for a review]. However, due to the technical difficulties of large-scale base space diagonalization and the excessive number of parameters (32), progress on the theoretical side was slow. To date, the application of the sdg-model has been restricted primarily to deformed nuclei, where this need is particularly acute. In order to deal with the main basic problem, various approximation schemes were used, e.g. truncating the base either to a maximum of one g-boson [20] or using an SU(3) basis [21]. Another solution has been the method of analytical  $1/N$  expansion [22], which is particularly suitable for deformed nuclei with

\*Corresponding author: prof.lai2014@gmail.com

DOI :10.21608/ejphysics.2021.54891.1061

Received : 23/12/2020; accepted : 25/1/2021

©2022 National Information and Documentaion Center (NIDOC)

**$N > 10$**  . For transitional nuclei where boson numbers are relatively smaller ( **$N > 10$** ), exact diagonalization will be preferred, and in larger mainframes it is still possible. The aim of this paper is to perform such an exact analysis using the computer code SDGBOSON [23], and to illustrate that it is possible to address the above-mentioned problems within a restricted set of parameters.

Classes of sdg-model Hamiltonians suggested by an analysis of shapes [24] to be acceptable for the isotopes of the Os are discussed in Sect.2. The dependency of parameters on various physical quantities is studied in order to limit the number of parameters in a physically realistic way. For feature calculations in this region, the systematics provided in this section would be useful. From a sect. 3, in the calculation of Os isotopes, these ideas are used. The emphasis here is on those properties of E2 and E4 that require the explicit introduction of g-boson for understanding.

*The sdg-Interacting Boson Model (sdg- IBM1)*

The Interacting Boson Model (IBM) suggests that the observed properties of the nuclei’s low-lying collective states emerge from the interplay of two effects: firstly, the strong interaction between identical particles (proton-proton and neutron-neutron); secondly, the strong interaction between quadrupole-quadrupole and non-identical particles (proton-neutron). The Interacting Boson Model (IBM) assumes that the even-even nucleus consists of an inert core plus some valence particles, which tend to pair together in states with angular momentum  $J = 0$  and  $J = 2$ , outside the closed shells at 50, 82, 126, and called s-bosons and d-bosons respectively, these pairs are treated as bosons. The total number of bosons  $N$  in a given nucleus is the proton,  $N_\pi$

and neutron sum  $N_\nu$ . The number of bosons is always half the number of nucleons of valence (or holes) counted from the nearest shell that is closed

$N = N_\pi + N_\nu$ . Between protons and neutrons, no distinction is made, therefore called IBM-1.

In the few past years considerable experimental data on E4 matrix elements and strength distributions has accumulated and their theoretical understanding (using models or microscopic theories) is a challenging problem. One of the models well suited for this purpose is the sdg-interacting boson model (sdg-IBM or simply gIBM); here the IBM with  $s (l = 0)$  and  $d (l = 0)$  bosons is extended to include  $g (l = 0)$  bosons.

For a practical study of experimental results, the sdg-model requires far too many parameters (32 in total). Therefore the application of the model depends on identifying a simple set of parameters which capture the essential physics. We are driven in this process by a recent study of shapes [24] which showed that I one-body terms control the transition from spherical to deformed shape but do not affect the degree of freedom of  $\gamma$ , (ii) odd multipole interactions do not play a role in shapes (iii) quadrupole interaction always leads to an axial shape, except that when the diagonal terms disappear ( $q_4 = 0$ ), resulting in a  $\gamma -$  unstable shape, (iv) stable triaxial shapes that are  $\gamma -$  soft can be obtained for some hexadecapole interaction choices. The points above imply that the shape of a Hamiltonian is [4]:

$$H = \varepsilon_g n_g + \kappa_1 L.L + \kappa_1 Q.Q + \kappa_4 T_4.T_4 \dots (1)$$

The description of transitional nuclei should be adequate. Here are given by the different multipole operators [4]:

$$n_g = \sum_{\mu} g_{\mu}^{+} g_{\mu} \dots \dots \dots (2)$$

$$L_{\mu} = \sqrt{0} [d^{+} d^{-}]_{\mu}^{(1)} + \sqrt{6} [g^{+} g^{-}]_{\mu}^{(1)} \dots \dots \dots (3)$$

$$Q_{\mu} = [s^{+} d^{-} + d^{+} s^{-}]_{\mu}^{(2)} + q_2 [d^{+} d^{-}]_{\mu}^{(2)} + q_4 [d^{+} g^{-} + g^{+} d^{-}]_{\mu}^{(2)} + q_4 [g^{+} g^{-}]_{\mu}^{(2)} \dots (4)$$

$$T_{4\mu} = [s^{+} g^{-} + g^{+} s^{-}]_{\mu}^{(4)} + h_2 [d^{+} d^{-}]_{\mu}^{(4)} + h_4 [d^{+} g^{-} + g^{+} d^{-}]_{\mu}^{(4)} + h_4 [g^{+} g^{-}]_{\mu}^{(4)} \dots \dots (5)$$

This Hamiltonian contains 10 parameters i.e., the single g-boson energy,  $\mathcal{E}_g$ ,  $\mathcal{K}_1$ ,  $\mathcal{K}_2$ , and  $\mathcal{K}_4$ , which are the strength parameters for the dipole, quadrupole and hexadecapole interactions, and the  $q_\beta$  and  $h_\beta$  quadruple and hexadecapole parameters. Although the number of free parameters is significantly smaller, a further reduction would be desirable.

First, we consider a special case of Eq.(1) with  $q_2 = q_4 = \mathcal{K}_4 = 0$  which has a  $\gamma$ -unstable energy surface and thus preserves the O(6) limit's successful characteristics, such as the well-known O(5) selection rule  $\Delta\tau = \pm 1$  for the transitions of E2 [25]. To illustrate this approximate realization of the symmetry of O(5) in the model of sdg.

Both the successful features of the O(6) limit and its failures resulting from the  $\gamma$ -unstable nature of its energy surface are shared by the above choice of the Hamiltonian. The inclusion of a hexadecapole interaction, as indicated in (iv) above, as in Eq.(1) could contribute to a triaxial shape that is  $\gamma$ -soft. However, phenomenological determination of the parameters of the

hexadecapole  $h_\beta$  poses a problem as the E4 data is rather scarce. To avoid parameter proliferation, we determine from a commutation condition that ensures that the mean fields of quadrupole and hexadecapole are coherent [22]. That is, we are

imposing  $[h^-, q^-] = 0$  that yields:

$$h_{22}^- = q_{24}^-, h_{24}^- = q_{44}^-, h_{44}^- = q_{24}^- + (q_{44}^- - q_{22}^- q_{24}^- + 1) / q_{24}^- \dots\dots\dots (6)$$

where  $q_{\beta\beta}^- = \langle j00|Q|20\rangle q_\beta$  and  $h_{\beta\beta}^- = \langle j00|Q|40\rangle h_\beta$ . When  $q_{22} = q_{44} = 0$ , Eq. (6) gives  $h_{22}^- = q_{24}^- = 0$ ,  $h_{24}^- = 0$ ,  $h_{44}^- = q_{24}^- - 1 / q_{24}^- \dots\dots\dots (7)$

The Hamiltonians considered in the previous paragraphs showed how in the sdg-model with a limited number (4-5) of parameters, various shortcomings of the O(6) limit could be rectified. A common feature of these Hamiltonians is that the selection rules for E2 are preserved and therefore the non-vanishing quadrupole moments observed in transitional nuclei are not described.

This clearly requires the condition  $q_2 = q_4 = 0$ , in the quadrupole operator Eq.(4) to be relaxed. In the following, with a general quadruple operator, we consider the Hamiltonian (Eq.(1)) but with the

hexadecapole parameters still determined from the condition Eq.(6). In addition, we will continue to use the consistent operators E2 and E4 [5,6,7]:

$$T^{(E2)} = e_2 Q \quad \text{and} \quad T^{(E4)} = e_4 T_4 \quad \dots\dots\dots (8)$$

No new parameters are added in the determination of electromagnetic transitions, so that, apart from the effective charges  $e_2$  and  $e_4$ .

To summarize the above systematic studies, it is possible to explain the E2 and E4 properties in the Hamiltonian with a general quadrupole and a coherent hexadecapole operator if  $\mathcal{K}_4 < 0$ . While the staggering systematics implies a positive  $\mathcal{K}_4$ , such an option ruins the excellent explanation of the properties of E2 and is not favored. Obviously, a simultaneous solution to all the problems noted in the introduction necessitates easing one of the conditions of coherence or constancy. This will create new parameters that we would rather stop.

**Results and Discussion**

*Energy Spectra*

Using the insights gained in the previous section, we now proceed to perform fits to the Os data. We do not try to fit each individual nucleus in depth here but we emphasize the overall pattern instead. The number of variable parameters is held to a minimum in this way. However as a result, we foresee some small differences between the calculated and experimental data. Furthermore, since the energy of the g-boson state ( $K^\pi = 4^+$  band) in the transitional region is almost constant,

the  $\mathcal{K} / \mathcal{E}_g$  ratio is almost constant. In each isotopic chain, it is held roughly constant. The

three parameters ( $\mathcal{K}_1, \mathcal{K}_2, \mathcal{K}_4 / \mathcal{E}_g$ ) are primarily correlated with the lowest-lying bands. On the other hand, the quadrupole parameters are modified to suit the transitions of E2 and E4. The parameters are indicated in Table 1.

Here we examine the <sup>188-194</sup>Os for which E4 data is available. Figures 1 - 4 display the determined spectrum for Os in sdg-IBM1 and experimental results, visibly improving the agreement between the calculated and experimental level schemes. This occurs because the isotopes of the Os are more deformed and the undesired effects of the  $\gamma$ -unstable limit on the quasi- $\beta$  and quasi- $\gamma$  band

energies are thus greatly reduced. The lower lying  $4^+$  (g-boson) state that requires smaller g-boson energy is another major change (see Table (1)). The mixing of the g-boson in the sd-states is therefore greater in the Os isotopes and is predicted to play a more important role in low-lying spectroscopy.

The  $R = E(4_1^+)/E(2_1^+)$  ratios are especially significant as the transition rotor ( $O(6)$  rotor) progresses, with the exception of the range from 3.077 to 2.634. From the energy spectra results, we see the  $K^\pi = 4^+$  in the  $^{190-194}\text{Os}$  isotopes are and are well described. But for  $^{188}\text{Os}$  isotope, the  $K^\pi = 4^+$  band-head energy levels are greater than the experimental 0.05 MeV. In general, the energy of the first excited ( $0_2^+$ ) state is high, as this state is perceived as the band head of the beta band. Instead of spherical nuclei, the yrast band spectra are identical to those of deformed nuclei. The second excited state of ( $0_3^+$ ) states decays primarily to  $2_2^+$  states in  $^{188-190}\text{Os}$ .

It is found that the sgd-IBM1 does not integrate high-spin states into calculations. The calculated levels of energy are always higher than experimental levels, and the discrepancies increase as one goes up to higher-spin states. It has been shown that when g-bosons are used in IBM, the calculated energy levels for higher spin states will be lowered. It is also assumed that the g-boson must be used if we intend to integrate high-spin states into the calculations.

#### Electric Transition Probability

The determined E2 matrix elements are compared in Table 3 with the available

experimental data of  $^{188-192}\text{Os}$ . From the transition  $B(E2; 2_1^+ \rightarrow 0_1^+)$  (normalized to experimental  $B(E2; 2_1^+ \rightarrow 0_1^+)$  value), the boson effective charges is given in Table 3. We see this effective charges re vary smoothly from isotope to another. The determined E2 matrix elements generally agree well with the data especially for the stronger E2 transitions which correspond to those permitted by the  $O(6)$  limit selection rule  $\Delta\tau = \pm 1$ . While differences remain in detail, the weaker transitions that would be forbidden at the  $O(6)$  limit are relatively well described. Remember that in a systematic study of smoothly changing parameters, these deviations from the calculated values are not constant (i.e., sometimes smaller and sometimes larger) and are thus not easily rectified. For the E2 transitions from the  $2_3^+$  state of Os isotopes, the most glaring difference exists. The determined values are an order of magnitude smaller than those observed, resulting from the persistence of the  $O(6)$  limit  $\Delta\sigma = 0$  selection law. To address this problem, more theoretical work on more efficient ways of breaking the  $O(6)$  symmetry is required. Also it would be desirable to shed more light on systematics with further experimental analysis of the E2 transition from the  $\sigma = N - 2$  levels.

In the Table 4, a comparison between sgd-IBM1 and experimental data for E2 matrix elements is shown. Again with less variations compared to the experimental values, the average agreement is much higher. Worth noting here are the E2 transitions from the  $4_3^+$  (g-boson) state that are fairly well explained. If the g-bosons were weakly coupled, these transitions would be minimal, and such a good explanation would not have been practicable.

TABLE 1. Sdg-IBM1 Hamiltonian Parameters for Os isotopes (in MeV units).

Isotopes	$N$	$\mathcal{E}_s$	$\mathcal{K}_1$	$\mathcal{K}_2$	$\mathcal{K}_4$
$^{188}\text{Os}$	10	0.620	0.005	-0.041	-0.014
$^{190}\text{Os}$	9	0.530	0.0125	-0.033	-0.012
$^{192}\text{Os}$	8	0.500	0.015	-0.030	-0.011
$^{194}\text{Os}$	7	0.450	0.015	-0.035	-0.010

TABLE 2. Effective charges in ( $e.b$ ) Units for  $^{188-194}\text{Os}$  isotopes.

Isotopes	$^{188}\text{Os}$	$^{190}\text{Os}$	$^{192}\text{Os}$	$^{194}\text{Os}$
$e_2$ ( $e.b$ )	0.129	0.136	0.143	0.151

TABLE 3. Reduced Matrix Elements for electric transition probability for Os isotopes.

Isotopes	Transitions	Exp. $\left  \langle J_f^+ \  T^{(E2)} \  J_i^+ \rangle \right $	sdg-IBM1 $\left  \langle J_f^+ \  T^{(E2)} \  J_i^+ \rangle \right $
<sup>188</sup> Os	$2_1^+ \rightarrow 0_1^+$	$1.584 \pm 0.022$	1.582
	$4_1^+ \rightarrow 2_1^+$	$2.646 \pm 0.057$	2.521
	$6_1^+ \rightarrow 4_1^+$	$3.257 \pm 0.109$	3.244
	$8_1^+ \rightarrow 6_1^+$	$3.950 \pm 0.329$	3.820
	$2_2^+ \rightarrow 2_1^+$	$0.866 \pm 0.023$	0.984
	$2_2^+ \rightarrow 0_1^+$	$0.483 \pm 0.010$	0.371
	$0_2^+ \rightarrow 2_1^+$	$0.077 \pm 0.029$	0.144
	$4_2^+ \rightarrow 4_1^+$	$1.098 \pm 0.09$	1.210
	$4_2^+ \rightarrow 2_2^+$	$1.775 \pm 0.113$	1.633
	$4_2^+ \rightarrow 2_1^+$	$0.283 \pm 0.018$	0.0044
	$6_2^+ \rightarrow 6_1^+$	$1.442 \pm 0.406$	1.261
	$6_2^+ \rightarrow 4_2^+$	$2.456 \pm 0.274$	2.500
	$6_2^+ \rightarrow 4_1^+$	$0.127 \pm 0.025$	0.334
	$4_3^+ \rightarrow 4_2^+$	$1.643 \pm 0.246$	0.611
	$4_3^+ \rightarrow 2_2^+$	$0.837 \pm 0.149$	0.855
	<sup>190</sup> Os	$2_1^+ \rightarrow 0_1^+$	$1.539 \pm 0.013$
$4_1^+ \rightarrow 2_1^+$		$2.366 \pm 0.042$	2.371
$6_1^+ \rightarrow 4_1^+$		$2.970 \pm 0.515$	2.887
$8_1^+ \rightarrow 6_1^+$		$3.712 \pm 0.105$	3.710
$2_2^+ \rightarrow 2_1^+$		$1.095 \pm 0.030$	1.118
$2_2^+ \rightarrow 0_1^+$		$0.456 \pm 0.012$	0.455
$0_2^+ \rightarrow 2_2^+$		$0.387 \pm 0.032$	0.389
$0_2^+ \rightarrow 2_1^+$		$0.118 \pm 0.011$	0.123
$4_2^+ \rightarrow 4_1^+$		$1.439 \pm 0.031$	1.500
$4_2^+ \rightarrow 2_2^+$		$1.871 \pm 0.040$	1.881
$4_2^+ \rightarrow 2_1^+$		$0.202 \pm 0.007$	0.221
$6_2^+ \rightarrow 6_1^+$		$1.766 \pm 0.184$	1.788
$6_2^+ \rightarrow 4_2^+$		$2.598 \pm 0.156$	2.601
$6_2^+ \rightarrow 4_1^+$		$0.194 \pm 0.090$	0.199
$4_3^+ \rightarrow 4_2^+$		$1.578 \pm 0.113$	1.580
$4_3^+ \rightarrow 3_1^+$		$1.543^{+0.091}_{-0.340}$	1.600
$4_3^+ \rightarrow 2_2^+$		$0.775 \pm 0.065$	0.709
$4_3^+ \rightarrow 2_1^+$		$0.052 \pm 0.006$	0.060
$4_3^+ \rightarrow 4_1^+$	$\approx 0.199$	0.221	

TABLE 3. Cont.

$^{192}\text{Os}$	$2_1^+ \rightarrow 0_1^+$	$1.457 \pm 0.018$	1.466
	$4_1^+ \rightarrow 2_1^+$	$2.115^{+0.018}_{-0.038}$	2.210
	$6_1^+ \rightarrow 4_1^+$	$2.9^{+0.010}_{-0.8}$	2.890
	$8_1^+ \rightarrow 6_1^+$	$3.8^{+0.7}_{-0.5}$	3.611
	$2_2^+ \rightarrow 2_1^+$	$1.224^{+0.030}_{-0.016}$	1.321
	$2_2^+ \rightarrow 0_1^+$	$0.425^{+0.8}_{-0.014}$	0.432
	$2_2^+ \rightarrow 4_1^+$	$0.3^{+0.2}_{-0.0}$	0.352
	$0_2^+ \rightarrow 2_1^+$	$0.066^{+0.012}_{-0.013}$	0.075
	$0_2^+ \rightarrow 2_2^+$	$0.449^{+0.044}_{-0.056}$	0.450
	$4_2^+ \rightarrow 4_1^+$	$1.3^{+0.0}_{-0.0}$	1.330
	$4_2^+ \rightarrow 2_2^+$	$1.637 \pm 0.050$	1.700
	$4_2^+ \rightarrow 2_1^+$	$0.125^{+0.018}_{-0.010}$	0.128
	$4_2^+ \rightarrow 6_1^+$	$0.0^{+0.0}_{-0.8}$	0.410
	$6_2^+ \rightarrow 6_1^+$	$1.9^{+0.0}_{-0.0}$	1.451
	$6_2^+ \rightarrow 4_2^+$	$2.0^{+0.3}_{-0.012}$	2.930
	$6_2^+ \rightarrow 4_1^+$	$0.067 \pm 0.076$	0.064
	$4_3^+ \rightarrow 4_2^+$	$1.19 \pm 0.22$	1.220
	$4_3^+ \rightarrow 3_1^+$	$1.6^{+0.0}_{-0.3}$	1.66
	$4_3^+ \rightarrow 2_2^+$	$0.9^{+0.2}_{-0.3}$	0.777
	$4_3^+ \rightarrow 2_1^+$	$0.113^{+0.064}_{-0.046}$	0.115

Experimental data are taken from refs. [26, 27, 28]

In order to evaluate the quadrupole moment

for first and second excited states  $Q(2_i^+)$ , we depend on the following equation [30]:

$$Q_J = \left[ \frac{16\pi}{5} \right]^{1/2} \begin{bmatrix} J & 2 & J \\ -J & 0 & J \end{bmatrix} \langle J_J \| T^{(E2)} \| J_J \rangle \quad (9)$$

The parameters of the quadrupole operator (Eq.(3)) are given in Table 5, Which were evaluated with the available experimental values.

The quadrupole moments of the  $2_1^+$  and  $2_2^+$  states are shown Table 6, and agree well with the experimental values. The drop in the quadrupole moments with increasing spin, which was encountered in the Os isotopes. In Table 6, we show the quadrupole moment calculations up to high spins which predict a prolate-oblate shape transition around  $\mathbf{I} = \mathbf{14}$ . The available data have rather large error bars, and more precise

measurements extending to higher spins would be desirable.

Less complete is the E4 data on the Os isotopes. So far the (p,p') experiments have only been performed for  $^{192}\text{Os}$  [15], and the E4 data is fairly well described in this case. For

the  $E4(0_1^+ \rightarrow 4_3^+)$  transitions, the other E4

data comes from  $(\alpha, \alpha')$  experiments which are sensitive to the reaction details and are therefore less reliable. On the other hand, the

$E4(0_1^+ \rightarrow 4_1^+)$  transitions are extracted from the more reliable (e,e') experiments, and are reproduced in the calculations quite well.

The E4 transitions that are one of the main motives for the present study are discussed. Since in each isotope there are only a few transitions



known, we tend to hold the effective charge constant for all Os isotopes at  $e_4 = 0.0343 \mathbf{b}^{-2}$ , calculated from fitting the  $^{192}\text{Os}$  transition  $0_1^+ \rightarrow 4_1^+$ . Table (7) compares the matrix

elements of the E4 determined using the consistent E4 operator (Eq.(8)) with the experimental data available. The overall agreement between the calculations and different measurements is excellent, provided that the E4 operator is derived from that of E2.

TABLE 4. Quadrupole parameters in (e.b) Units for Os isotopes.

Isotopes	$q_2$	$q_3$	$q_4$
$^{188}\text{Os}$	-0.240	0.900	0.50
$^{190}\text{Os}$	-0.262	0.900	0.50
$^{192}\text{Os}$	-0.281	0.900	0.50
$^{194}\text{Os}$	-0.300	0.900	0.50

TABLE 5. Quadrupole moments (e.b) Units for Os isotopes.

Nuclei	$J_i^+$	Exp.	sdg-BM1
$^{188}\text{Os}$	$2_1^+$	-1.46(4) <sup>a</sup>	-1.540
	$2_2^+$	1.00(25) <sup>b</sup>	1.033
$^{190}\text{Os}$	$2_1^+$	-1.18(3) <sup>c</sup>	-1.201
	$2_2^+$	0.9(4) <sup>c</sup>	0.998
$^{192}\text{Os}$	$2_1^+$	-0.96(3) <sup>d</sup>	-0.887
	$2_2^+$	-0.8(3) <sup>d</sup>	-0.91
$^{194}\text{Os}$	$2_1^+$	-	-0.878

a- [26]    b- [27]    c- [28]    d-[29]

TABLE 6. E4 matrix elements for Os isotopes in  $\mathbf{b}^{-2}$  Units.

Isotopes	$E4(0_1^+ \rightarrow 4_1^+)$		$E4(0_1^+ \rightarrow 4_2^+)$		$E4(0_1^+ \rightarrow 4_3^+)$	
	Exp.	sdg-IBM1	Exp.	sdg-IBM1	Exp.	sdg-IBM1
$^{188}\text{Os}$	0.217(11) <sup>a</sup>	0.214	-	0.185	0.109 <sup>c</sup>	0.111
$^{190}\text{Os}$	0.212(12) <sup>a</sup>	0.210	-	0.160	0.078 <sup>c</sup>	0.089
$^{192}\text{Os}$	0.220(10) <sup>a</sup>	0.223	0.116(29) <sup>b</sup>	0.112	0.108(27) <sup>c</sup>	0.106
$^{194}\text{Os}$	-	0.224	-	0.101	-	0.100

a- [14]    b-[15]    c-[10]

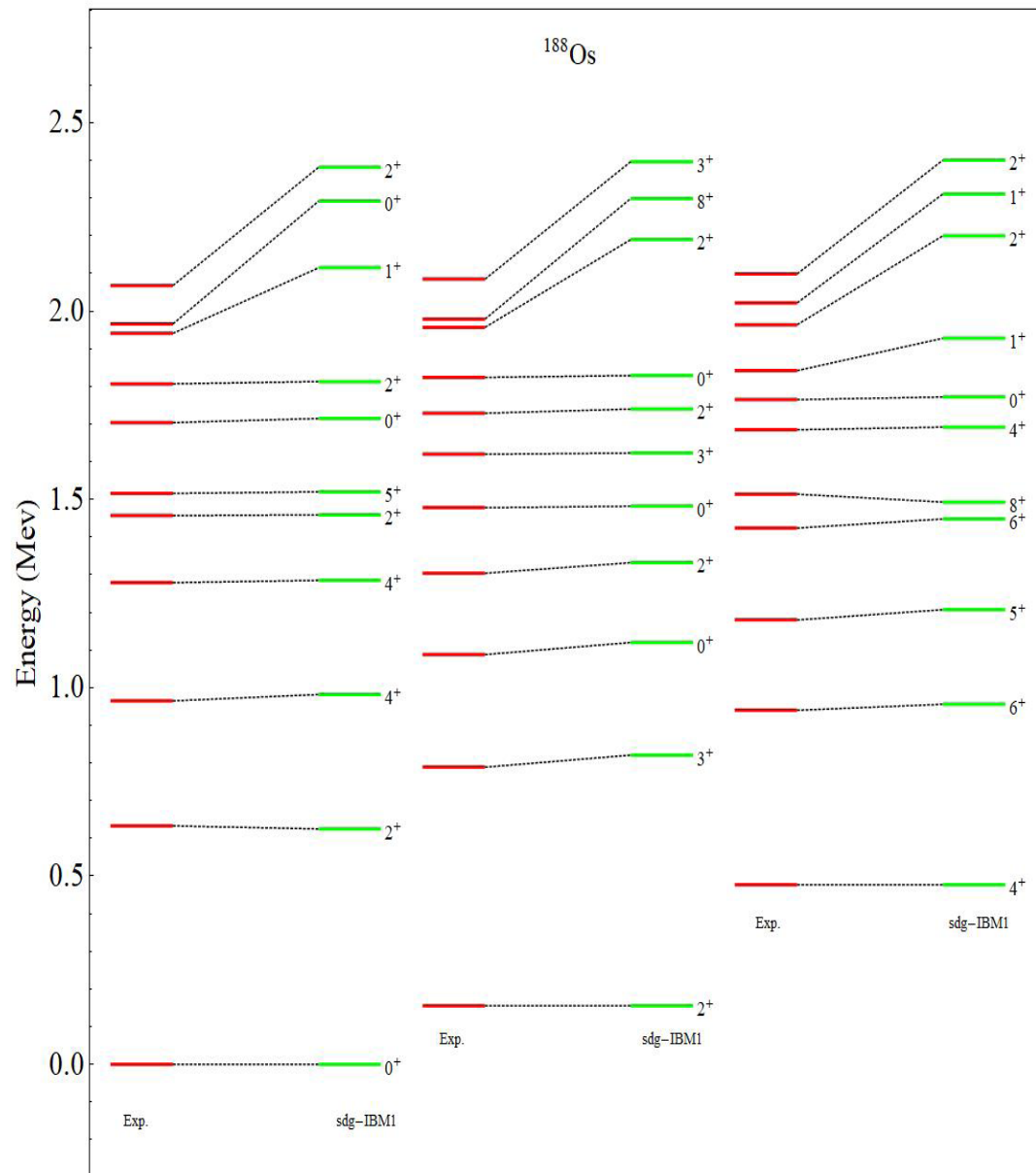


Fig. 1. Comparison between experimental data [26] and IBM-2 calculated energy levels for  $^{188}\text{Os}$  isotope.



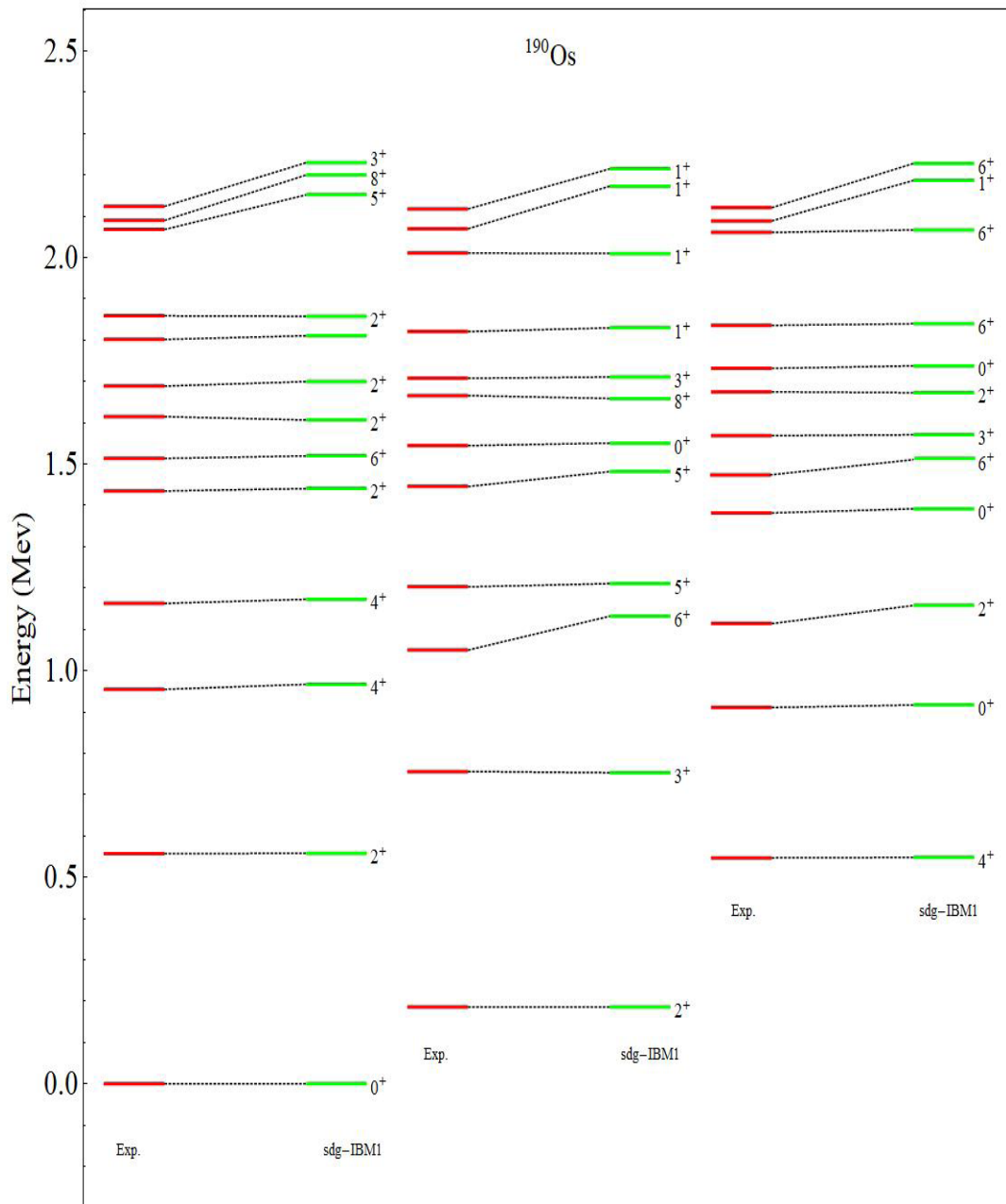
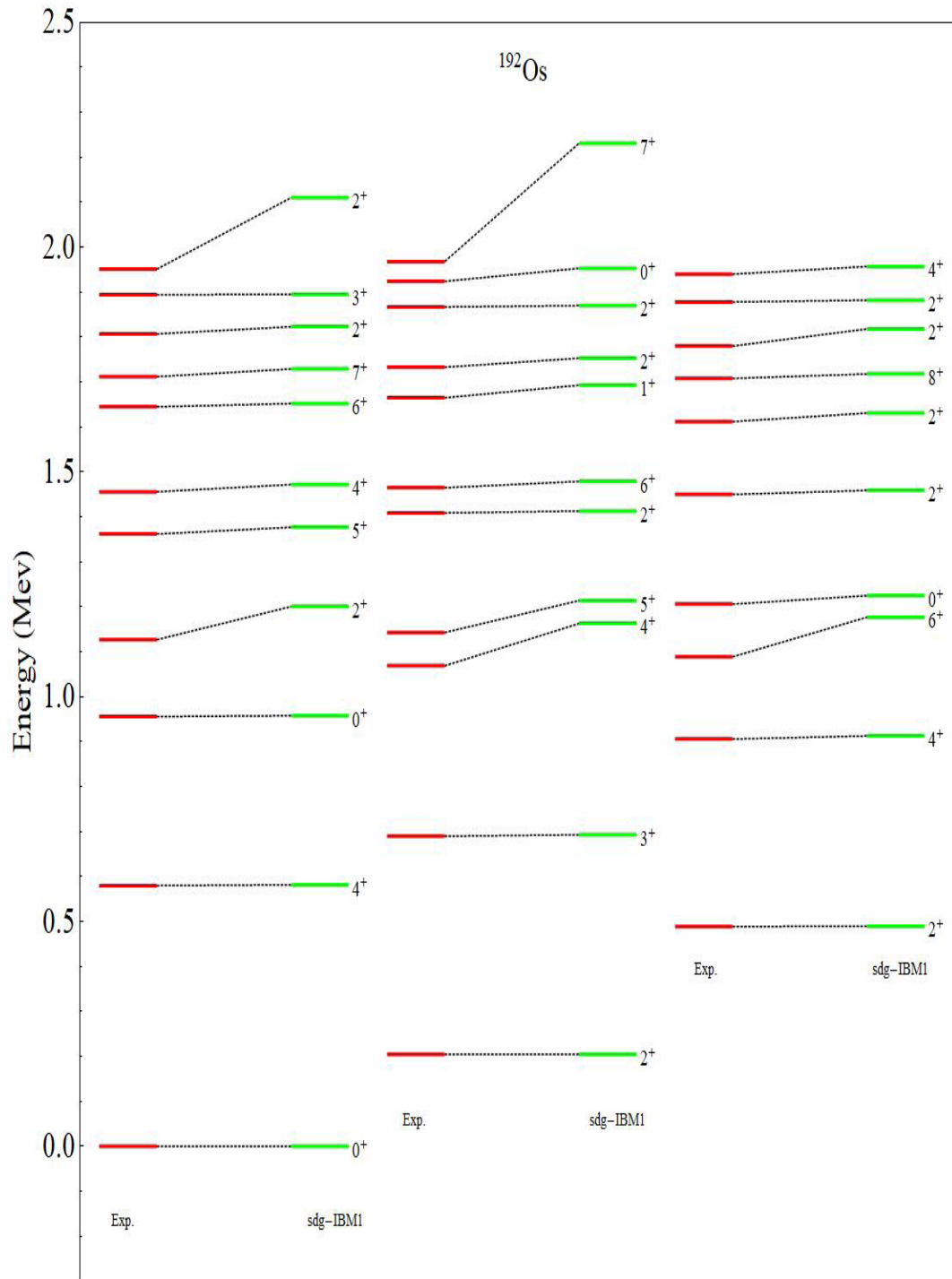


Fig. 2. Comparison between experimental data [27] and IBM-2 calculated energy levels for  $^{190}\text{Os}$  isotope.



**Fig. 3.** Comparison between experimental data [28] and IBM-2 calculated energy levels for  $^{192}\text{Os}$  isotope.

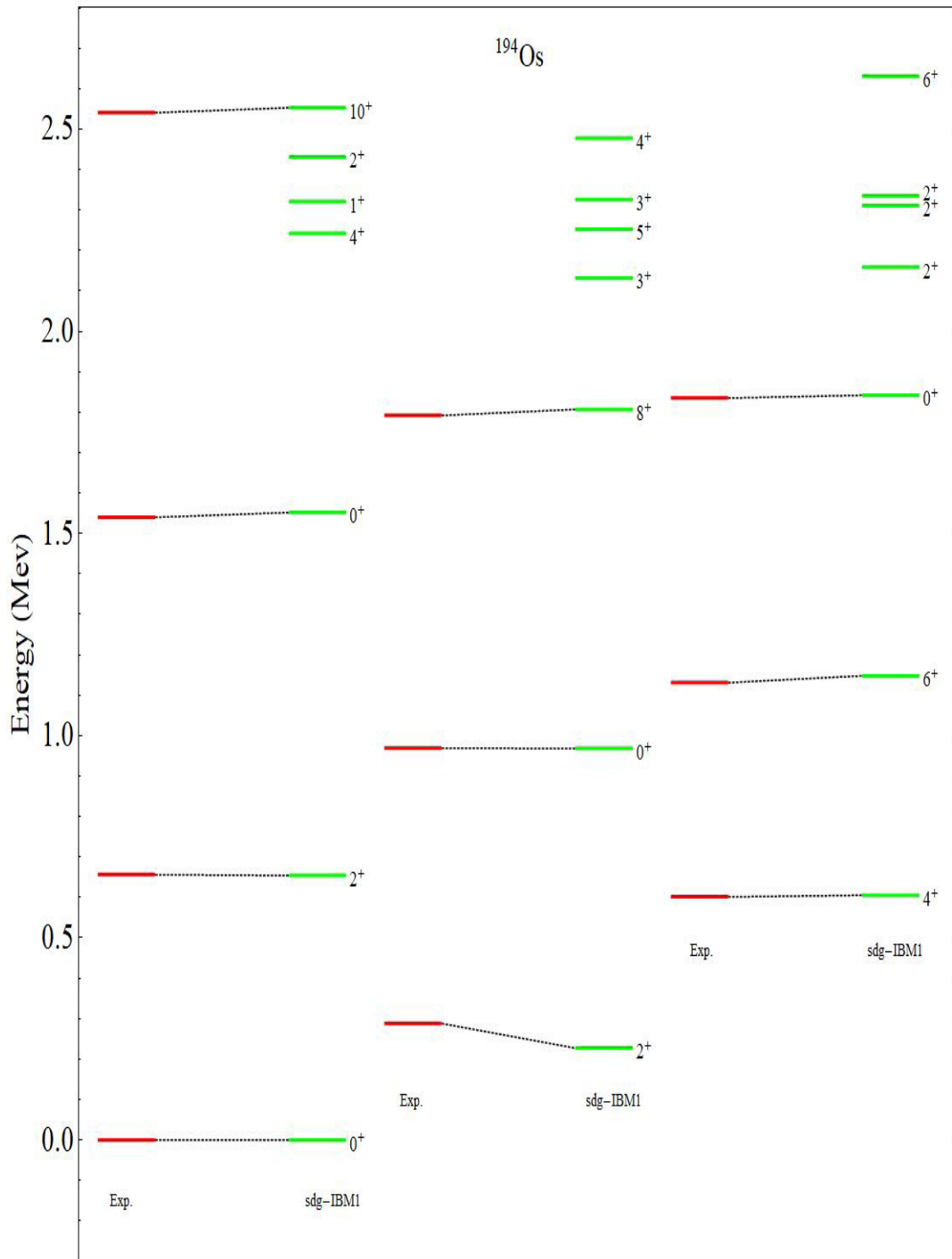


Fig. 4. Comparison between experimental data [29] and IBM-2 calculated energy levels for  $^{194}\text{Os}$  isotope.

### Concluding Remarks

In this study, we have discussed some special features of the sdg-boson model that are important to the transitional nuclei description. In particular, we have shown how a quadrupole Hamiltonian can achieve the  $\gamma$ -unstable limit and how a coherent hexadecapole interaction can induce  $\gamma$ -soft triaxiality. In more general terms, we have also considered the Hamiltonian model and have established systematic patterns for different physical quantities of interest. The number of free parameters is an overbearing concern in the sdg-model. We have limited this number to nine (7 in the Hamiltonian and two effective charges) by different consistency and coherence conditions, which are often kept constant or change smoothly within an isotopic chain. This approximately doubling of the parameters relative to the sd model is well justified given that 30-40 pieces of data are clarified for each nucleus. It should also be emphasized that some of the E2 and E4 data, irrespective of the number of parameters used in the sd-models, cannot be represented without g-bosons.

In summary, a coherent overview of the E2 and E4 properties in the Os using a restricted set of parameters, isotopes were obtained. The problems with the transitions of quadrupole moments, yrast E2 and E4, which cannot be clarified in the sd-models, have been resolved satisfactorily. The complex shape transitions that could be checked with the new  $4\pi$ -detector systems “Euroball” and “Gamma-Sphere” are an important prediction of the current calculations.

### References

- 1.A .S. Davydov and G.F. Filippov, *Nucl . Phys .* **8** (1958) 237
2. L . Willets and M . Jean, *Phys. Rev.* **102** (1956) 788
3. G . Gneuss and W . Greiner, *Nucl. Phys.* **A171** (1971) 449 ; P.O . Hess, J.Maruhn and W. Greiner, *J . of Phys.* G7 (1981) 737 .
4. F. Iachello and A . Arima, *The interacting-boson model* (Cambridge Univ . Press, Cambridge, 1987)
5. R.F. Casten and D.D . Warner, *Rev. Mod. Phys.* **60** (1988) 389
6. R.F. Casten and J.A . Cizewski, *Nucl.Phys.* A309 (1978) 477 ; *Phys. Lett.* B185 (1987) 293
7. R.F. Casten, P . von Brentano, K . Heyde, P . van Isacker and J .Jolie, *Nucl . Phys.* **A439** (1985) 289
8. M.P. Fewell *et al.*, *Phys. Lett.* B157 (1985) 353 ; M.P. Fewell, *Phys. Lett.* **B167** (1986) 6
- 9.A . Mauthofer *et al.*, *Z. Phys.* A336 (1990) 263
- 10 .D.G . Burke, M.A.M . Shahabudin and R. N . Boyd, *Phys. Lett.* 78 (1978) 48.
- 11.F. Todd Baker *et al.*, *Phys. Rev.* **C17** (1978) 1559
12. P.T . Deason *et al.*, *Phys. Rev.* **C23** (1981) 1414
13. W.T.A . Borghols *et al.*, *Phys. Lett.* **B152** (1985) 330
14. W . Boeglin *et al.*, *Nucl . Phys .* A477 (1988) 399
15. F. Todd Baker *et al.*, *Nucl . Phys .* A501 (1989) 546
16. A . Sethi *et al.*, *Nucl . Phys .* A518 (1990) 536
17. A . Sethi *et al.*, *Phys. Rev .* C44 (1991) 700 [18] A . Sethi, Private communication, (2020)
19. R . Bijker, A.E.L . Dieperink, O. Scholten and R . Spanhoff, *Nucl . Phys .* A344 (1980) 207.
- 20.P. Van Isacker, K. Heyde, M . Waroquier and G . Wenes, *Nucl. Phys.* A380 (1982) 383.
21. N . Yoshinaga, Y . Akiyama and A . Arima, *Phys . Rev .* C38 (1988) 419.
22. S.Kuyucak and I.Morrison, *Ann.Phys.(NY)***181**(1988)79; S. Kuyucak, I . Morrison and T . Sebe, *Phys . Rev.* **C43** (2019) 1187.
23. I. Morrison, Computer code SDGBOSON, (University of Melbourne, 1986).
24. S. Kuyucak and I. Morrison, *Phys. Lett.* **B255** (1991) 305.
25. S. Kuyucak, V.-S. Lac, I. Morrison and B.R. Barrett, *Phys. Lett.* B263 (1991) 347
26. Balraj Singh, *Nuclear. Data Sheets* **95** (2002) 413.
27. Balraj Singh, *Nuclear. Data Sheets* **99** (2003) 285.
28. Coral M. Baglin, *Nuclear. Data Sheets* **113** (2012) 1883.
29. Balraj singh, *Nuclear. Data Sheets* **107** (2006) 1537.
30. A. Bohr and B.R. Mottelson: “Nuclear Structure”, Vol. II, (W.A. Benjamin, Reading, Massachusetts, 1975).